Heliyon 9 (2023) e15874

Contents lists available at ScienceDirect

Heliyon

journal homepage: www.cell.com/heliyon

Research article

The use of pracaxi oil collector in the selective flotation of xenotime from silicates

Rafaella Lúcia Martins [a], Luciano Fernandes de Magalhães [a], Leandro Henrique Santos [b], Gilberto Rodrigues da Silva [c,*]

[a] Postgraduate Program in Metallurgical, Materials and Mining Engineering, Federal University of Minas Gerais, MG, Brazil
[b] Department of Mining and Civil Construction, Federal Centre of Technological Education of Minas Gerais, MG, Brazil
[c] Department of Mining Engineering, Federal University of Minas Gerais, MG, Brazil

ARTICLE INFO

Keywords:
Rare earth
Xenotime
Surface characterization
Flotation
Novel collector
Pracaxi oil

ABSTRACT

Rare earth elements have played a key role in technological advancement, attracting great visibility in the global commodity market. Xenotime, a heavy rare earth resource (YPO_4), can be found associated with granitic rocks, as in the Pitinga deposit, located in the Brazilian Amazon region, where the main gangue minerals are quartz, microcline and albite. This research investigates the application of a new collector produced from pracaxi oil, an Amazon oil abundant in Brazil, in the selective flotation between xenotime and its main gangue minerals. The study conducted the synthesis and characterization of the collector, the chemical, mineralogical and surface characterization of minerals, as well as the evaluation of collector adsorption and flotability via microflotation tests, zeta potential measurements, surface tension determination and XRD, WDXRF, ICP-MS, FTIR and XPS analyses. The pracaxi collector was found to be mainly composed of oleic acid (56.2%), linoleic acid (14.1%) and behenic acid (10.6%), in addition to exhibiting a critical micelle concentration (CMC) of approximately 150 mg/L. Microflotation tests indicated that the best condition for selective recovery of xenotime occur at alkaline condition (pH 9.0), presenting selectivity of approximately 90% with collector concentration of 10.0 mg/L. The zeta potential data confirmed a selective adsorption of pracaxi collector onto xenotime, with an increase in the surface charge from −30 mV to −68 mV, whereas no significant changes were detected in the silicates. The FTIR spectra showed the appearance of a band at 1545 cm^{-1} on the surface of the xenotime after collector adsorption, which indicates, along with the zeta potential data, the chemical nature of the adsorption. The presence of small amounts of iron in the lattice structure of silicate gangues can act as an activator, and therefore, may be responsible for the small flotability of these minerals. The performance of the pracaxi oil collector presented in this study indicates the great potential of this Amazonian oil for application in the selective flotation of xenotime ores found in the region.

1. Introduction

Rare earth elements (REE), an indispensable raw material in high technology industries, have attracted significant visibility in the

* Corresponding author.
E-mail address: grsilva@demin.ufmg.br (G. Rodrigues da Silva).

https://doi.org/10.1016/j.heliyon.2023.e15874
Received 20 April 2022; Received in revised form 27 March 2023; Accepted 24 April 2023
Available online 28 April 2023

world market after a reduction in global supply in recent years [1]. In this scenario, many countries around the world have found themselves under pressure to localize and process alternative rare earth resources, reducing their external dependence and developing their own industry [2]. Most REE resources are associated with three main minerals: bastnaesite ($(Ce,La)CO_3F$) and monazite ($(Ce,La,Nd,Th)PO_4$), for light rare earths, and xenotime (YPO_4), for heavy rare earth [3]. Despite its great importance, recent research into new routes for concentration of rare earth resources has focused on bastnaesite and monazite, with little effort being devoted to processing xenotime ores [4]. This mineral is found associated with pegmatites and, in Brazil, it is described as one of the by-products of cassiterite ore in the albite-granite deposit exploited by Mineração Taboca [5]. In this mineral deposit, located in Pitinga, in the Amazon region, the main gangue minerals present are quartz (SiO_2) and feldspars, mainly albite ($NaAlSl_3O_8$) and microcline ($K(AlSi_3O_8)$ [6].

According to Jordens et al. [7], flotation is one of the main methods applied for the concentration of rare earth ores, as it allows the processing of fine particles and is adaptable to the mineralogy of the deposit. A variety of collectors for rare earth flotation have been studied, including: fatty acids, hydroxamates, dicarboxylic acids and phosphoric acids [7]. Fatty acids, especially sodium oleate, have been reported in the literature as collectors used in the flotation of phosphate [8], rare earth minerals [9], fluorite, calcite and apatite [10–12] among other minerals, and this class of reagents usually is the first option investigated in the flotation of rare earth minerals, due to its relatively low cost and high availability [13]. The efficiency of fatty acids (Aero 704, Sylfat FA2) in rare earth flotation is reported in the literature by studies carried out with xenotime and monazite, with silicate minerals and hematite as gangue, which showed great recovery of rare earth minerals (about 70%), whereas gangue minerals could not be recovered [14]. Fatty acids were also used at the Weishan deposit in China, where oleic acid was applied to produce a concentrate containing more than 60% bastnaesite [4].

A more socially and environmentally sustainable approach to rare earth flotation could be the use of collecting reagents obtained from vegetable oils, which are rich in fatty acids and have high potential for selectivity [15]. The Amazon region stands out for its varied sources of vegetable oils, due to the great diversity of its flora [16], and whose exploitation by the cosmetics and food industries generates a large amount of oil-rich by-products [17]. The application of seeds, fruits or residues from renewable sources can shape the local economy to exploit native vegetation, preserving it and avoiding deforestation. Recent studies have indicated great potential for the application of amazon oils in the synthesis of collectors for phosphate flotation [18,19].

The collectors obtained from the saponification of vegetable oils are systems composed of different fatty acids in varying proportions, which can present synergy when applied in flotation [19]. The synergistic action of mixed collectors, when used in ideal proportion, has the advantage of combining the individual characteristics of each component, providing greater coverage of the mineral surface and changes in the foam characteristics, increasing its stability [19]. This fact is attributed to the impact that the mixture generates on the critical micelle concentration (CMC) and on the interfacial tension (TI), which are lower than those observed for each individual component [20]. Thus, the synergy between collectors can lead to higher mineral recovery, greater adsorption of the main collector component on the mineral surface and superior selectivity [12]. Octohydroxamic acid (OHA) and sodium oleate (NaOL), for example, were used as mixed collectors to reduce cost, increase recovery and maintain selectivity for bastnaesite flotation. The results indicated an increase in bastnaesite recovery by 33% when compared to an individual use of OHA under the same conditions [21].

The application of pracaxi oil (Pentaclethra macroloba) in mineral flotation has not yet been investigated to date, although the amazon oil presents great potential for the production of collectors due to its specific acid profile, with a high concentration of behenic acid (19%), in addition to containing a large amount of oleic acid and lignocenic acid [22]. The present research investigates the use of the fatty acid salt obtained from pracaxi oil as a selective anionic collector in the flotation of xenotime from its main gangue minerals in granitic deposits.

2. Experimental

2.1. Materials

Samples of xenotime, albite, microcline and quartz were purchased for the analyses conducted in this study. The xenotime sample was acquired from Cristais Aquarius (BR), whereas the other mineral samples were acquired from Luiz Menezes Comércio e Exportação de Minerals Ltd. (BR). The samples were manually ground, with the aid of a mortar and pestle, up to a particle size range of -150 μm $+$ 38 μm, for microflotation and XPS tests. This size range was chosen considering previous studies on xenotime flotation using fatty acids and the need to avoid entrainment of fine particles [23]. A portion of these particles was further pulverized to -38 μm, to be used in XRD, FTIR and zeta potential measurements. Pracaxi oil (PXO) samples were acquired from the Amazon Oil Co. (BR) for synthesizing the pracaxi oil collector (PXC).

2.2. Methods

2.2.1. Mineralogical and chemical characterization

The phase composition of each sample was evaluated by X-ray powder diffraction (XRPD) analyses in a PW1710 diffractometer (Philips-PANalytical, UK) equipped with copper X-ray source ($\lambda\kappa\alpha = 1.54$ Å) and graphite monochromator crystal, and performed at 50 kV and 35 mA, with 2θ ranging from 3 to 90°, step size of 0.06° (2θ) and scan time of 3 s. Rietveld refinement method was used to calculate the purity of the samples based on the phases identified. The chemical composition of the samples was examined via wavelength dispersive X-ray fluorescence (WDXRF) on a PW2404 spectrometer (Philips-PANalytical, UK), inductively coupled plasma optical emission spectrometry (ICP-OES) using an Optima spectrometer 7300DV (PerkinElmer, US) and inductively coupled plasma mass spectrometry (ICP-MS) using a Nexion 300X spectrometer (PerkinElmer, US). Sample preparation consisted of fusion with

$Li_2B_4O_7$, for WDXRF, and, for ICP-MS/ICP-OES, multi-acid plate digestion at 230 °C, with sample/solution ratio 1 g: 10 mL, for quartz, or fusion with $LiBO_2$ at 950 °C with a sample/flux ratio of 1 g: 10 g, for the other mineral samples.

2.2.2. Pracaxi oil/collector synthesis and characterization

The characterization of the pracaxi oil sample was performed by determining its iodine index, acid index and saponification degree via direct method, according to ASTM D5554-15, ASTM D5555-95 and ASTM D5558-95 standards, respectively. The determination of the fatty acid profile of the sample was obtained using gas chromatography in an HP7820A gas chromatograph (Agilent, US) equipped with a flame ionization detector. The synthesis of the collector was carried out via saponification of pracaxi oil in a reflux system, aiming to improve the solubility of long chain molecules present in the oil. The saponification was performed by reacting the pracaxi oil with NaOH solution (0.5 mol/L) at 75 °C, for a period of 1 h. In this reaction (Fig. 1), the triglycerides present in the oil sample were broken down with the aid of the alkali, forming glycerol and fatty acid salts, which were the collector molecules used in the flotation experiments. Different fatty acid salts were obtained since the triglycerides are of natural origin. After saponification, the product was filtered and oven dried at 80 °C for 18 h. The saponification efficiency was evaluated by analyzing the oil and saponified products via Fourier transform infrared spectroscopy (FTIR). In this test, an Alpha II spectrometer (Bruker, DE) was used in Attenuated Total Reflectance (ATR) mode, using diamond crystal, 32 scans and readings between 4000 and 400 cm^{-1} with 4 cm^{-1} resolution.

To determine the Critical Micellar Concentration (CMC) of the pracaxi oil collector, surface tension measurements were conducted using the Du Nouy ring technique in a K10ST tensiometer (Krüss, DE). The experiments were conducted at a temperature of approximately 21 °C and in an alkaline medium, pH 10.0 (±0.1). For the elimination of organic contaminants, the platinum ring was flame treated prior to each measurement.

2.2.3. Zeta potential

The electrical properties of the mineral particles were studied by electrophoresis, using a Particle Analyzer ZM3-D-G (Zeta Meter, US), with subsequent calculation of the Zeta Potential. The mineral samples below 38 μm were used. The test was performed conditioning the mineral samples with electrolyte solution and electrolyte + collector solutions. For sample conditioning, 0.5 g of mineral was added to 100 mL of KCl solution (10^{-3} mol/L). The collector concentration used during the tests was 10 mg/L. Samples were conditioned for 3 min, followed by sedimentation for 1 min. The supernatant was collected and inserted into the cell. Measurements were performed at pH 5.0, 7.0 and 9.0, using NaOH and HCl solutions for pH adjustment.

2.2.4. Microflotation

Microflotation tests were conducted in duplicate in a modified Hallimond tube (310 mL), using a height extender to avoid hydrodynamic drag. In each test, 0.5 g of each mineral, with particle size between 150 μm and 38 μm, was used, varying the collector concentration and pH of the system. The mineral particles were conditioned with the collector for 3 min, air was injected into the cell at a flow rate of 40 $cm^3\ min^{-1}$ and flotation was conducted for 1 min. Floated and sunken fractions were collected, filtered and oven dried for subsequent weighing. The tests were performed in three pH ranges: acidic (pH 5.0), neutral (pH 7.0) and basic (pH 9.0), with collector concentrations of 1 mg/L, 5 mg/L and 10 mg/L. The chosen pH range has been pointed as the best range in previous studies on xenotime flotation with fatty acid salts [25].

2.2.5. Surface characterization

The surfaces of the xenotime, microcline, quartz and albite samples were investigated after conditioning under the optimal conditions of the microflotation tests, with and without the presence of PXC. The study began with X-ray Photoelectron Spectroscopy (XPS), using an AMICUS monochromatic X-ray photoelectron spectrometer (Kratos Analytical, UK) equipped with a Mg κα X-ray source (1253.6 eV). Elemental surveys were carried out from 0 to 1200 eV (resolution: 1 eV, residence time: 100 ms), whereas the high-

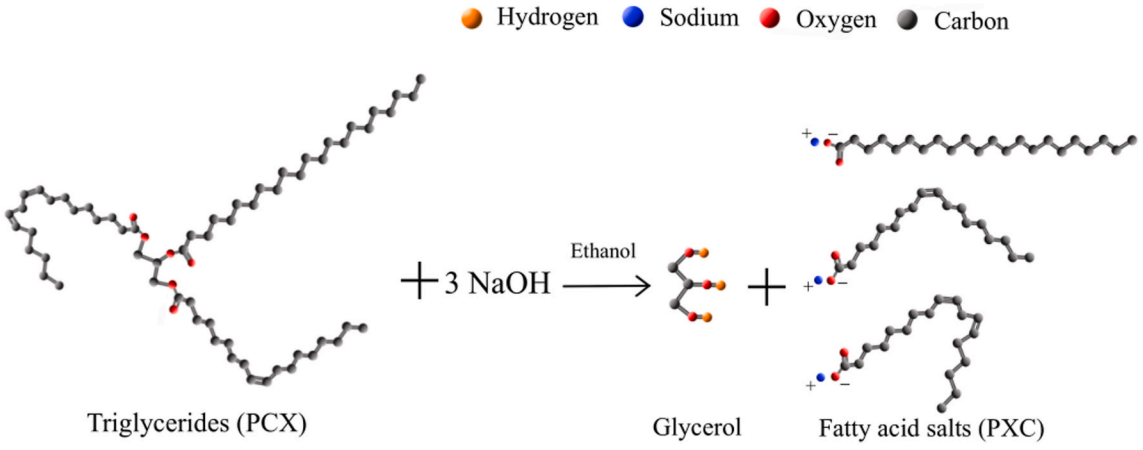

Fig. 1. PXO saponification reaction (alkaline hydrolysis) (Adapted from Ref. [24]).

resolution spectra were obtained using a pass energy of 0.1 eV. After conditioning in solutions at optimum flotation pH, the samples were dried at room temperature and degassed for 6 h in a forced-air oven at room temperature and kept in a vacuum desiccator before the experiments. The results were fitted using the Vision Processing software (Kratos Analytical, UK) and the C 1s peak for C–C was used as the standard (BE at 284.8 eV) for shift correction. The study of the mineral surfaces, before and after conditioning with the collector, was also carried out via Attenuated Total Reflectance Fourier Transform Infrared Spectroscopy (ATR-FTIR), under the equivalent operational conditions used in the PXO and PXC characterization. In this analysis, mineral samples below 38 μm were extensively pulverized, aiming to increase the specific surface area and the collector-mineral interaction signal.

3. Results and discussion

3.1. Mineralogical and chemical characterization

The crystalline phase composition of mineral samples, determined by XRD, are shown in the difractograms in Fig. 2.

The XRD analysis indicates that the samples present high purity, confirmed by the Rietveld refinement, which indicated 100% purity for quartz, xenotime and albite samples. As for the microcline sample, a 10% albite impurity was detected.

The chemical analyses (Table 1) indicate the presence of impurities in quantities below the detection limit of X-ray diffraction. Iron was detected as the main contaminant (743 ppm) in the quartz sample. In the xenotime sample, in addition to yttrium, other rare-earth elements are present in small amounts, such as dysprosium (Dy_2O_3 – 2.73%), erbium (Er_2O_3 – 1.63%), gadolinium (Gd_2O_3 – 1.44%) europium (Eu_2O_3 – 1.3%) and holmium (Ho_2O_3 – 1.19%). The microcline ($K(AlSi_3O_8)$) and albite ($Na(AlSi_3O_8)$) samples present similar composition, as both belong to feldspar group, and differ by the proportion of potassium oxide (K_2O) and sodium oxide (Na_2O). These samples also showed contamination with Fe_2O_3, present as 0.59% in the microcline and 0.29% in the albite sample.

3.2. Pracaxi oil/collector synthesis and characterization

Table 2 shows the results obtained in the gas chromatography test for pracaxi oil, as well as the data informed by Amazon Oil [22] and Heppard et al. [26].

The PXO fatty acid profile is in agreement with the data provided by Amazon Oil Co., and is compatible with characterization studies carried out with pracaxi oil, showing the predominance of oleic (C18:1), followed by linoleic (C18:2), and behenic acid (C22:0) [26]. However, a small difference can be observed between the values obtained in this work and those presented in the literature, as indicated by the differences in the proportions of lignoceric (C24:0), stearic (C18:0) and palmitic acid (C16:0). Climatic factors directly influence the development of plants, which modify the composition of vegetable oils. According to Heppard et al. [26], it is expected an inversely proportional relation between the amount of polyunsaturated fatty acids present in vegetable oils and the temperature at which plant development occurs.

The chemical parameters of pracaxi oil are shown in Table 3. The saponification value, which can indicate the size of hydrocarbon chains in fatty acids present in the sample, and iodine value, which refers to the degree of unsaturation of these acids, are in agreement to the data provided by Amazon Oil Co [22]. The iodine index (72.2 g $I_2.g^{-1}$) demonstrates a high degree of unsaturation in the collector. This index is considered an indicator of the flotation efficiency and selectivity of fatty acids, being indicated as one the

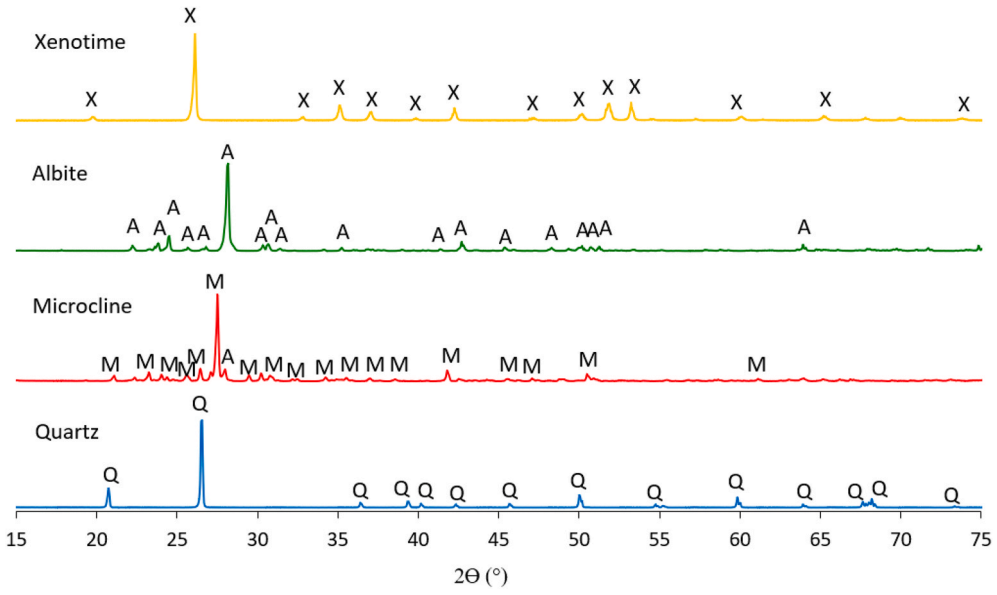

Fig. 2. X-ray diffractogram of the mineral samples. Phases identified: X - xenotime, A - albite, M - microcline and Q - quartz.

Table 1
Chemical analysis of xenotime, albite, microcline and quartz samples.

Sample	Chemical composition														
Xenotime	**Y_2O_3**	**P_2O_5**	**Dy_2O_3**	**TiO_2**	**Yb_2O_3**	**Al_2O_3**	**Er_2O_3**	**Gd_2O_3**	**CaO**	**Eu_2O_3**	**Ho_2O_3**	**Nd_2O_3**	**Fe_2O_3**	**K_2O**	**SiO_2**
	%	%	%	%	%	%	%	%	%	%	%	%	%	%	%
	46.17	33.84	2.73	2.6	2.15	2.13	1.63	1.44	1.35	1.3	1.19	1.12	0.28	0.05	0.4
Microcline	**SiO_2**	**Al_2O_3**	**K_2O**	**Na_2O**	**Fe_2O_3**	**P_2O_5**	**MnO**	**CaO**	**MgO**	**Ba**	**Tl**	**Ga**	**Sr**	**Ni**	**-**
	%	%	%	%	%	%	%	%	%	ppm	ppm	ppm	ppm	ppm	–
	62.86	16.47	13.7	1.46	0.59	0.07	0.06	0.05	0.03	105	18.2	18.1	12	13	–
Albite	**SiO_2**	**Al_2O_3**	**Na_2O**	**$F_{e2}O_3$**	**CaO**	**K_2O**	**MgO**	**P_2O_5**	**Cr_2O_3**	**Ta**	**Sr**	**Zn**	**Ba**	**Nb**	–
	%	%	%	%	%	%	%	%	%	ppm	ppm	ppm	ppm	ppm	–
	67.5	17.88	10.83	0.29	0.26	0.23	0.04	0.03	0.02	347.63	87	40	35	25.47	–
Quartz	**SiO_2**	**Fe**	**Al**	**Ca**	**Li**	**K**	**Na**	**Mn**	**Ti**	**Mg**	**Zn**	**P**	–	–	–
	%	ppm	ppm	ppm	ppm	ppm	ppm	ppm	ppm	ppm	ppm	ppm	–	–	–
	99.71	743	134	60	12	10	10	9	8	7	3	2	–	–	–

Table 2
Comparative analysis of pracaxi oil fatty acid profile.

Fatty acid	C12:0	C14:0	C16:0	C18:0	C18:1	C18:2	C18:3	C22:0	C24:0
Sample	0.2	0.2	3.7	4.1	56.2	14.1	0.2	10.6	4.9
Amazon Oil Co. [22]	0.8–1.8	1–1.8	1.5–3	1.5–3	40–50	1.8–3.0	2–4	18–21	13–16
Heppard *et al.* [26]	–	–	1.53	2.68	53.46	12.22	0.11	16.54	11.13

Table 3
Chemical parameters of pracaxi oil.

Chemical parameter	Direct method	Amazon Oil Co.
Saponification Value (mg KOH.g^{-1})	176.0	175.0–188.0
Acidity Index (mg KOH.g^{-1})	10.3	<10.0
Iodine Value (g I_2.g^{-1})	72.2	50.0–77.0

features responsible for the greater selectivity and flotability presented by linoleic acid (C18:2) over oleic acid (C18:1) in pyrophyllite flotation [27]. This parameter also refers to the oxidative stability of oils, and high values indicate good quality and longer shelf life of the vegetable oil [15]. The saponification index of pracaxi oil (176 mg KOH.g^{-1}), when compared to other Amazonian oils, such as patauá oil (190 mg KOH.g^{-1}), can be considered low, indicating that pracaxi oil presents higher molecular weight and also longer hydrocarbon chains [28]. The presence of long hydrocarbon chain molecules results in more effective hydrofobization of particles, which may be positive in to achieve high recoveries with lower collector dosages. The acidity index indicates the proportion of free fatty acids in the composition of oil samples. High acidity levels represent advantages in the saponification process, as free fatty acids favor the occurrence of primary fatty acid salts that act as catalysts [18]. The acidity index of pracaxi oil (10.3 mg KOH.g^{-1}) indicates a lower saponification potential in comparison to other Amazonian oils, such as patauá, which presents indexes between 28 and 43 mg KOH.g^{-1} [18,19].

To evaluate the efficiency of pracaxi oil saponification, ATR-FTIR analyses were conducted on samples before and after the process, in order to identify the most significant bands related to the fatty acids' hydrocarbon chains, carboxylates and alcohols (ethanol and glycerol). As indicated in Fig. 3, it is possible to observe the characteristic bands of pracaxi oil and the differences after the saponification process. In both spectra, an increase in the characteristic bands of glycerides (1.744 cm^{-1}) and alcohol (3.355 cm^{-1}, 1.047 cm^{-1}, 1.650 cm^{-1}) is noticeable, which is explained by the use of alcohol in the saponification process [19]. The characteristic bands of triglycerides and free fatty acids (1.743 cm^{-1} and 1.710 cm^{-1} in Fig. 3A, respectively) were replaced by a band at 1.558 cm^{-1} (in Fig. 3B), characteristic of fatty acid sodium salts, indicating complete saponification of the pracaxi oil sample [19]. The bands at 2.922 cm^{-1} and 2.852 cm^{-1} correspond to the C–H elongation vibration of the –CH_2– and –CH_3 groups, respectively [29].

The characterization of PXC was also carried out by measuring its influence on surface tension at different concentrations, at pH 9.0, with results shown in Fig. 4. The increase in the collector concentration leads to a reduction in the surface tension of the solution, demonstrating the inversely proportional relation of these quantities and the strong tensoactive action of the collector. The premicellar concentration (PMC) and the critical micellar concentration point (CMC) were determined to be at approximately 15 mg/L and 150

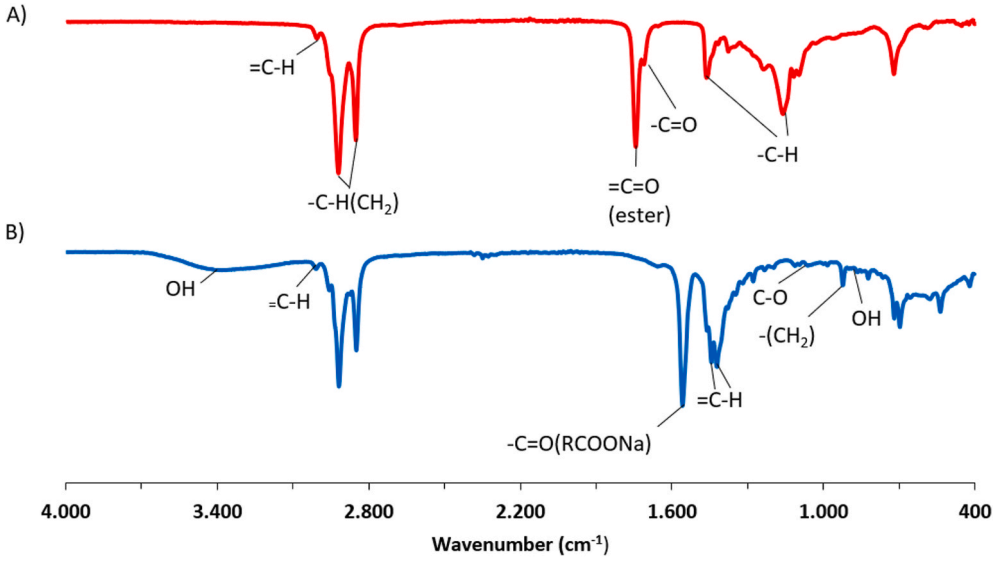

Fig. 3. ATR-FTIR spectra of (A) pracaxi oil (PXO) and (B) pracaxi oil collector (PXC).

mg/L, respectively. In this concentration range, the formation of hemi-micelles occurs with the adsorption of the collector species at the solid/liquid interface, making the particle surface hydrophobic and favoring flotation [30].

The investigation conducted by Oliveira et al. [19] to assess the surface tension of another Amazonian collector, produced from pataua oil for phosphate flotation, demonstrate CMC below 100 mg/L, similar to the value found for pracaxi in the present study (150 mg/L). Investigations with sodium oleate have showed that the collector can present CMC values up to 300 mg/L, demonstrating the influence of the fatty acid profile of Amazonian oils on the activity their respective collectors and on their CMCs, which may indicate synergies between the different acid molecules present in mixed collectors [19,20].

3.3. Microflotation

The graphs in Fig. 5 show the results of xenotime, quartz, microcline and albite microflotation as a function of PXC concentration and pH. The results shown in Fig. 5A indicate that, under alkaline conditions (pH 9.0), larger selectivity can be achieved between xenotime and the silicate minerals. No significant difference in the flotability of the three gangue minerals is observed. Studies have already indicated similarities in the surface properties of feldspars and quartz in flotation systems with anionic collectors and the need for activating cations to recover these minerals [31]. The low floatability shown by quartz, microcline and albite could be explained with the data from the chemical analysis, shown in Table 1, which shows high degree of purity of these mineral samples. The small floatability, nevertheless, can be attributed to the iron and aluminum present in the crystalline structure of mineral samples, which can act as activating sites at the particles' surface. The negative charge of silicate gangue minerals in a wide pH range indicate that the adsorption of fatty acids on iron sites occurs as a chemical adsorption, but other mechanisms proposed are ion exchange, neutralization of surface hydroxyl groups $Fe(OH)^{2+}$ by the fatty acid salt, or surface precipitation [32,33].

Analyzing the recovery of minerals as a function of PXC concentration, at pH 9.0 (Fig. 5B), it can be observed that great recovery of xenotime (80%) can be achieved using 5.0 mg/L PXC solutions, even with the surface tension data (Fig. 4) indicating the beginning of hemi-micelle formation at approximately 15 mg/L. These results may be related to the synergistic effect on adsorption of the different fatty acid molecules present in PXC, and show the high efficiency of the collector in the coverage of the mineral surface [20,34]. The adhesion step strongly depends on surface hydrophobicity, which is enhanced by longer hydrocarbon chains. In the case of PXC, the presence of behenic (10.6%) and lignocenic acid (4.9%), with 22 and 24 carbons atoms in the hydrophobic chain, respectively, can play this role, even in small collector concentrations. Besides, the stronger hydrophobic interaction of long carbon chain benefits the particles aggregation, which facilitates the recovery of fine particles [35]. Although errors in the measurement of surface tension and determination of PMC should not be ignored, the low concentrations required for selective flotation using mixed collectors from vegetable oils stand out in relation to classic collectors used individually. In previous research on xenotime flotation, sodium oleate concentrations greater than 100 mg/L were required to achieve similar performance to that of PXC, which represents concentrations at least 10 times higher than those presented in this study [31,36]. The greater efficiency of PXC may also be related to the high iodine index of pracaxi oil, which indicated that the synthesized collector would present a high degree of unsaturation, or the saponification value of the sample, which showed the presence of longer hydrocarbon chains, both characteristics that can result in greater chemical activity and selectivity in flotation [27].

Xenotime, like apatite, is a mineral from the phosphate group and may have similar surface characteristics. The high selectivity in the flotation xenotime with fatty acid salts observed in the present work was also noticed for apatite flotation with the use of fatty acid collectors, in studies carried out by Rao and Foessberg [37] e Moudgil et al. [13], and also proven in studies with xenotime and sodium oleate performed by Cheng et al. [36] and Anderson et al. [34].

The microflotation results show a small increase in the floatability of the silicate minerals with an increase in the concentration from 5 mg/L to 10 mg/L (Fig. 5B). This increase in concentration, however, is also followed by an increase in xenotime recovery, which

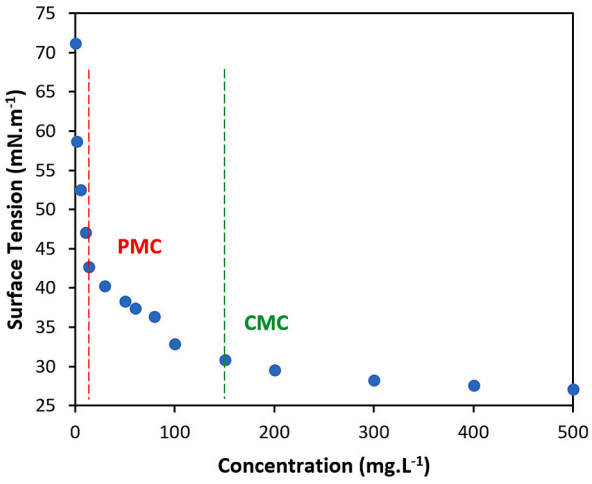

Fig. 4. The effect of PXC concentration on surface tension, at pH 9.0.

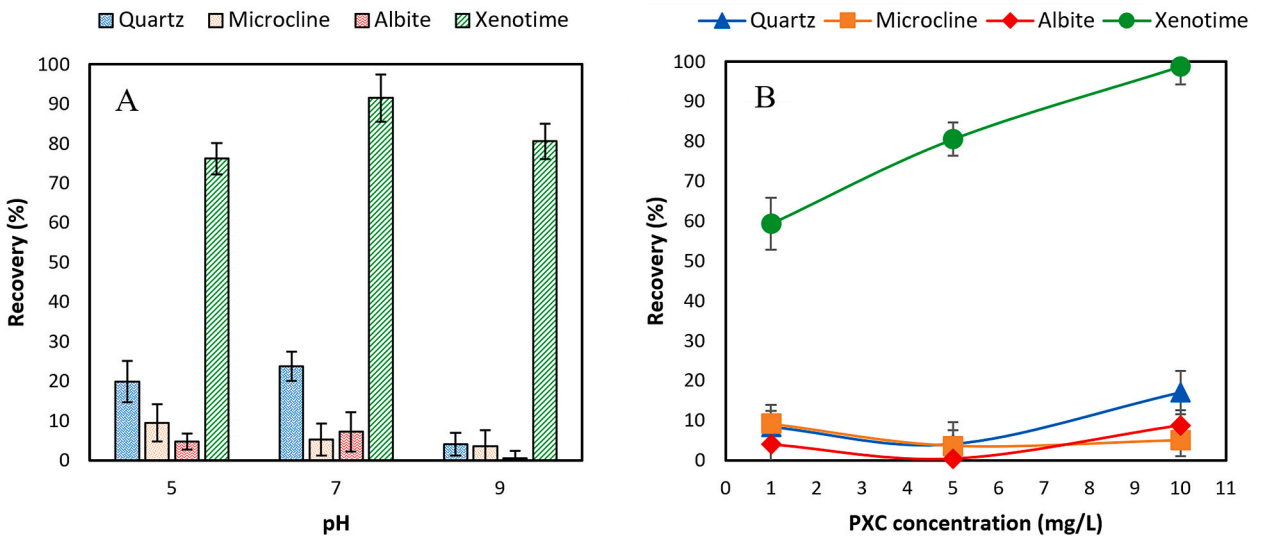

Fig. 5. Microflotation recovery of xenotime, albite, microcline and quartz as a function of (A) pH at 5 mg/L PXC and (B) PXC concentration at pH 9.0.

results in maximum mineral selectivity at 10 mg/L (99% xenotime recovery against average 10% silicates recovery), agreeing with observations made by Cheng et al. [25], which demonstrated a positive tradeoff to work with higher concentrations of sodium oleate, the sodium salt formed by acid oleic saponification. The authors correlated the vibrational acceleration of the bubble-particle system with pH and collector concentration, demonstrating that, at higher pH values and sodium oleate concentrations, a lower detachment of collector molecule from mineral surface is observed, favoring the flotation process [25]. Cheng et al. also demonstrates that collector adsorption onto xenotime surfaces strongly depends on the pH range, with recovery decaying in pH below 7 [36]. The authors used the sodium oleate stability diagram to explain this decay, which was attributed to the lesser presence of $RCOO^{-}$, $(RCOO)_2^{2-}$ and $(RCOO)_2H^{-}$ species at pH values below 7 [38].

Coulombic attraction and hydrophobic interaction are the main driving forces that characterize the adsorption process as physical phenomenon, whereas strong covalent or coordinated bonds between the collector and surface species is characterized as a chemical process [39]. As presented by Cheng et al., electrostatic interactions are frequently considered the main factors driving the adsorption of surfactants onto oxides and other non-metallic minerals, therefore, it would be anticipated that sodium oleate would physically adsorb onto xenotime [25]. However, since the xenotime surface is negatively charged above its point of zero charge (PZC), the authors mention that the expected recovery would be low, contrary to the 80% xenotime recovery observed, which indicates that the type of adsorption between the hydroxyl groups on xenotime surface [$RE(OH)^{2+}$] and sodium oleate could be of chemical nature, even in conditions with high electrostatic repulsion [36]. The results observed with PXC, with high recovery of xenotime at alkaline pH, also indicate that the adsorption is a chemical process. Nevertheless, in alkaline environment, the conversion of [$RE(OH)^{2+}$] into $RE(OH)_3$ also leads to less active sites for the adsorption of the pracaxi collector, which explains the reduction of floatability observed from pH 7 to pH 9 [36].

The technical and economic advantages in the use of mixed collectors have already been proposed [40]. The association of fatty acids found in the composition of Amazonian oils can lead to a synergistic effect, that is, an improvement in their efficiency when compared to the individual use of these acids. This phenomenon could explain the high flotability observed for xenotime even at concentrations as low as those of hemi-micelle formation. The synergistic effect is reported in several studies with different types of collectors (anionic, cationic and non-ionic) and for different types of ores (sulfide, coal and silicate) [41–43]. The best efficiency in the use of reagent mixtures is attributed to the decrease in CMC and surface tension [20]. According to Bradshaw et al. [41], the use of only one collector in flotation causes a non-uniform coverage on the mineral surface due to adsorption taking place only at strong sites, thus decreasing the adsorption density. This was possibly avoided in the experiments with PXC, at which different fatty acid salt molecules could facilitate the adsorption at different sites on the surface of xenotime. As indicated by the chemical analysis, other rare earth elements are present in smaller amounts in the sample, resulting in more diverse sites at the mineral surface. This greater diversity of molecules would help to have a more efficient coverage at low concentrations, even with the great diversity of sites expected for xenotime.

3.4. Zeta potential

Fig. 6 presents the zeta potential results for xenotime, quartz, microcline and albite samples in the presence and absence of PXC, in the pH range from 5.0 to 9.0. The data is consistent with the literature, which points out negative charge above PZC values between pH 2.3 and 5 for xenotime [25,34]. A decrease in the zeta potential of xenotime, from pH 7.0 to 9.0, was observed. Similar result has been

measured for monazite (Ce, La, Nd, Th)PO_4 [25] and might be related to the solubility of the metal and the speciation of system. A decrease in the zeta potential of xenotime at pH 9.0 is possible according to the speciation presented by Zhang and Anderson [34], which indicates the presence of YOH^{2+}, $Y_2(OH)_2^{4+}$, and $Y(OH)_2^{+}$ in solution at this pH condition. These species could adsorb on the xenotime particles, partially reducing their negative sites. As for feldspars, microcline and albite, and quartz, it has been shown that the PZC is found in acidic conditions, at approximately pH 2.0 [31], which is also consistent with the observations in Fig. 6.

The results show that, in the pH range investigated, all minerals show negative surface charge and that, for xenotime, there was a significant increase in the negative charge of the particles after conditioning with PXC at pH 9.0. The zeta potential of quartz, albite and microcline do not indicate adsorption of ionic species of the collector as no significant variations in zeta potential are observed after conditioning with PXC. The absence of significant modification in the zeta potential of silicates is consistent with the low recoveries observed in microflotation tests conducted in previous studies [44]. The authors demonstrate the need of activators for adsorption and flotation of these minerals with sodium oleate. The chemical analysis data (Table 1) indicate the presence of Fe as a contaminant in the crystalline structure of silicates. As discussed in section 3.3, the iron present in the crystalline lattice of mineral behave as active sites for adsorption of the pracaxi collector, which leads to small variations in zeta potential (Fig. 6) and low floatability (Fig. 5A and B). As PXC is an anionic collector, the significant reduction in the zeta potential of xenotime particles at pH 9.0 and the speciation diagram of oleic acid [10], main component of PXC, indicate that specific adsorption of $RCOO^{-}$ and $(RCOO)_2^{2-}$ species took place at the xenotime surface, in agreement with the chemisorption mechanism proposed for PXC and xenotime in section 3.3. The zeta potential observed at lower pH values is also in agreement with the speciation diagram, indicating the predominance of RCOOH species, which should play a significant role in flotation, although with lesser impact on the particles surface charge. The adsorption of this species can explain the xenotime recovery and also greater recovery of silicates at pH 5.0 and 7.0, as seen in Fig. 5A.

3.5. Surface characterization

3.5.1. XPS

The surfaces of xenotime, microcline, albite and quartz particles were analyzed using X-ray Photoelectron Spectroscopy (XPS), a technique widely used to characterize mineral surfaces [21]. The results are shown in Figs. 7 and 8.

The Si 2p spectra of quartz, albite and microcline samples were appropriately fitted with Gaussian peaks assigned to Si–O–Si [45–47] at 102.87, 102.52 e 102.67 eV, respectively. The O 1s spectra of these silicates (Fig. 7A, B and 7C) were fitted with a peak attributed to oxygen atoms present as oxides at 530.34, 530.63 and 530.70 eV, respectively, and a second peak attributed to Si–O–Si [45,47–49], at 532.14, 531.95 e 531.92 eV, respectively. The results indicated an increase in the presence of oxygen as oxide at the expense of Si–O–Si in the following order: quartz < albite < microcline. These results are consistent with the chemical analysis (Table 1), which indicates the presence of Fe as a contaminant as the binding energies of the oxide peaks are similar to values observed in O 1s spectra of Fe_2O_3. The small flotability of silicates can be credited to the occurrence of Fe oxides, which is consistent with adsorption of fatty acid salts in Fe_2O_3 sites.

The XPS spectra of the xenotime sample are shown in Fig. 8. The O 1s spectra (Fig. 8A) indicated the presence of metal oxide, xenotime and water physically adsorbed on particle surface, with binding energies at 529.74, 531.49 and 533 0.74 eV, respectively [49,50]. The P 2p spectrum (Fig. 8B) confirmed the major presence of xenotime sites on the sample surface [46], at 133.80 eV, and required the adjustment of a peak at 132.35 eV, which could be attributed to trisodium phosphate [48]. The Y 3d spectrum (Fig. 8C) was fitted with doublets assigned to YPO_4, as the 3d5/2 doublet was fitted with a Gaussian peak at 157.33 eV [51,52]. The sites observed for the xenotime sample are not different from those expected for the mineral, and do not indicate the presence of precipitates

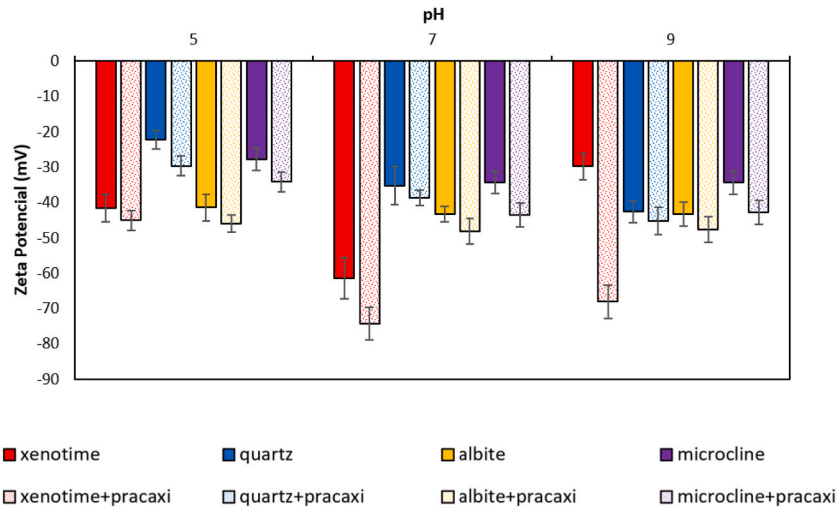

Fig. 6. Zeta Potential of xenotime, albite, microcline and quartz as a function of pH, with and without the presence of PXC.

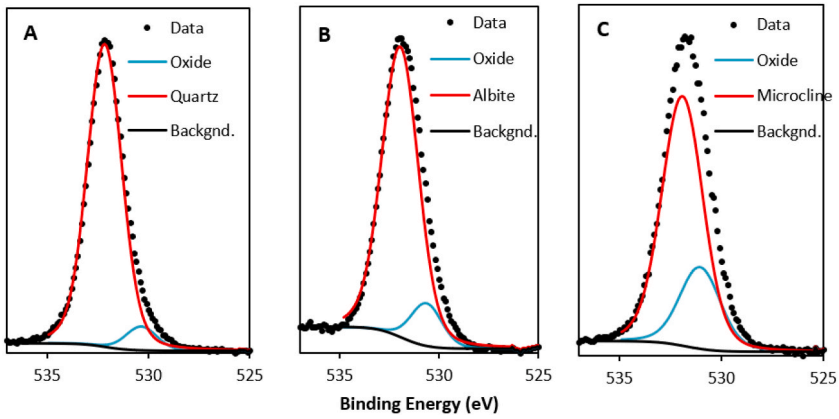

Fig. 7. O 1s XPS spectra of (A) quartz, (B) albite and (C) microcline, conditioned at pH 9.0.

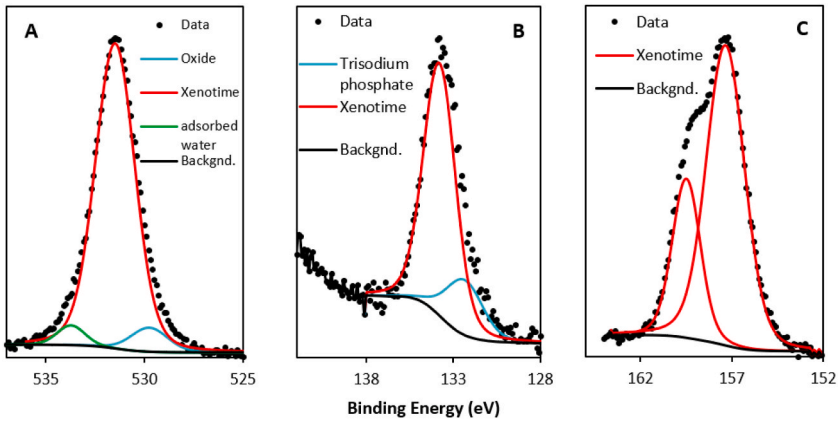

Fig. 8. (A) O 1s, (B) P 2p and (C) Y 3d XPS spectra of xenotime, conditioned at pH 9.0.

or other species resulting from mineral dissolution. The PXC adsorption and the mineral flotation must be associated, then, with the chemical adsorption on the sites of yttrium and other ETR identified in the chemical analysis of the xenotime.

3.5.2. FTIR

The ATR-FTIR spectra of xenotime, albite, microcline and quartz surfaces, before and after conditioning with PXC at pH 9.0, are shown in Fig. 9A, B, 9C and 9D, considering the wavenumber range between 2000 cm^{-1} and 400 cm^{-1}.

The spectra indicated that, after conditioning with PXC, new bands at 1471 cm^{-1} and 1420 cm^{-1} [19] can be observed, predominantly on xenotime surface (Fig. 9A), being attributed to hydrocarbon chain of fatty acid salts from the collector. These data corroborate with the zeta potential results, which suggest specific adsorption between PXC and xenotime, and with the high recovery observed in microflotation tests. Fig. 10 shows a comparison between detailed ATR-FTIR spectra with and without the conditioning of xenotime with PXC, with emphasis on the wavenumber range characteristic of carboxylates. It is possible to observe small bands at approximately 1545 and 1575 cm^{-1} [53], which indicates the occurrence of chemical adsorption of $(RCOO)_2^{2-}$ species at metallic site (yttrium or other ETR) in the surface of xenotime, corroborating the data presented in previous studies, which also show this band as evidence of chemical adsorption [18,19,39]. The sodium carboxylate band in the collector was observed at a lower wavenumber (1558 cm^{-1}), as indicated in the PXC spectrum (Fig. 3B), representing a shift of the carboxylate peak after adsorption on the mineral surface, which has also been observed by Oliveira et al. [19]. In the case of the silicate minerals (Fig. 9B, C and 9D), small peaks are observed at 1471 cm^{-1} and 1420 cm^{-1} bands, indicating a slight adsorption of PXC, which may justify the recoveries in microflotation tests, although it is not possible to indicate the presence of chemisorption, as no significant bands are observed at 1545 and 1575 cm^{-1}.

The chemisorption between xenotime and fatty acids was observed by Moudgil et al. [39]. Cheng et al. [36] indicated that the pH variation affects the major species in solution and at the mineral surface, causing different types of interactions at the solid-liquid interface. Luo et al. [54] and Fuerstenau [55] suggest that hydroxylated rare earth ions such as RE $(OH)^{2+}$ and RE $(OH)_2^{+}$ (predominant at pH < 10) can adsorb onto the mineral surfaces, forming activation centers. These sites, although not identified in the XPS O 1s spectrum (Fig. 8A), could also play a role in the chemisorption observed between PXC and the xenotime surface.

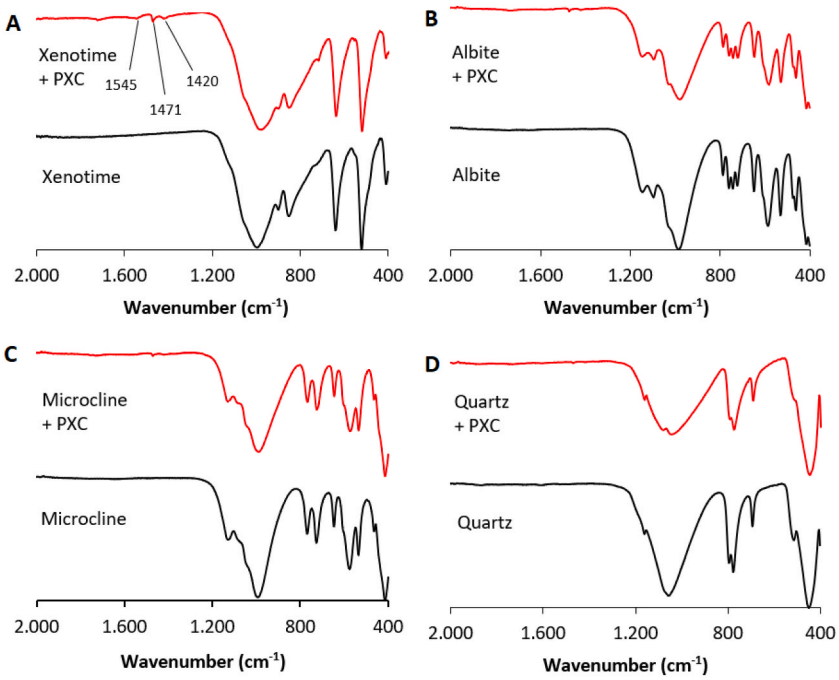

Fig. 9. ATR-FTIR spectra of (A) xenotime, (B) albite, (C) microcline and (D) quartz in the presence and absence of pracaxi oil collector (PXC) at pH 9.0.

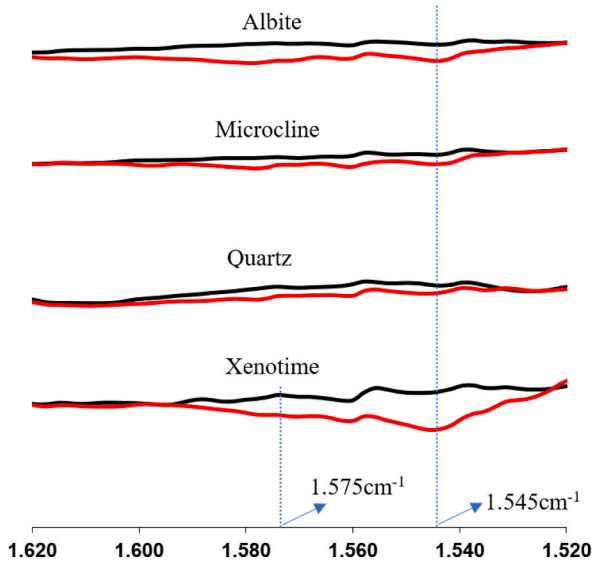

Fig. 10. Detailed ATR-FTIR spectra of xenotime, albite, microcline and quartz, before and after conditioning with PXC at pH 9.0.

4. Conclusions

This work investigated the potential of pracaxi oil collector (PXC) in the selective flotation of xenotime from the main silicate gangue minerals found in granitic deposits. Pracaxi oil is a renewable source of fatty acids, in addition to being found in abundance in the Amazon region. PXC is mainly composed of salts of oleic, linoleic and behenic acid, showing high recovery and selectivity at much lower concentrations (5 mg/L) than those observed for sodium oleate. The use of PXC as xenotime collector showed improved results at alkaline pH (pH 9.0), at which the surface charge (zeta potential) indicated the collector specific adsorption onto the xenotime surface, whereas FTIR spectra showed the appearance of a new 1.572 and 1.545 cm^{-1} bands, indicating a chemical contribution in the collector adsorption mechanism. The results also suggest that the presence of Fe contamination in silicate minerals can lead to surface

activation, with a decrease in the collector selectivity. This highlights the importance of the chemical and microstructural characterization of gangue minerals present in the ore. This study complements recent research demonstrating the potential of Amazonian oils in the development of new collectors and promoting the discussion on the adsorption mechanism of mixed collectors.

Author contribution statement

Rafaella Lúcia Martins: Conceived and designed the experiments; Performed the experiments; Analyzed and interpreted the data; Wrote the paper.

Luciano Fernandes de Magalhães: Conceived and designed the experiments; Analyzed and interpreted the data.

Leandro Henrique Santos: Analyzed and interpreted the data.

Gilberto Rodrigues da Silva: Analyzed and interpreted the data.

Funding statement

This work was supported by Pró-Reitoria de Pesquisa da Universidade Federal de Minas Gerais (UFMG), Programa de Pós-graduação em Engenharia Metalúrgica, Materiais e de Minas (PPGEM), Fundação de Amparo à Pesquisa do Estado de Minas Gerais (FAPEMIG), Conselho Nacional de Desenvolvimento Científico e Tecnológico (CNPq) and Coordenação de Aperfeiçoamento de Pessoal de Nível Superior (CAPES).

Data availability statement

Data included in article/supplementary material/referenced in article.

Declaration of competing interest

The authors declare that they have no known competing financial interests or personal relationships that could have appeared to influence the work reported in this paper.

References

[1] A. Jordens, C. Marion, R. Langlois, T. Grammatikopoulos, N.A. Rowson, K.E. Waters, Beneficiation of the Nechalacho rare earth deposit. Part 1: gravity and magnetic separation, Miner. Eng. 99 (2016) 111–122, https://doi.org/10.1016/j.mineng.2016.04.006.

[2] K. Binnemans, P.T. Jones, B. Blanpain, T. Van Gerven, Y. Pontikes, Towards zero-waste valorisation of rare-earth-containing industrial process residues: a critical review, J. Clean. Prod. 99 (2015) 17–38, https://doi.org/10.1016/j.jclepro.2015.02.089.

[3] Z. Zhu, Y. Pranolo, C.Y. Cheng, Separation of uranium and thorium from rare earths for rare earth production – a review, Miner. Eng. 77 (2015) 185–196, https://doi.org/10.1016/j.mineng.2015.03.012.

[4] C. Marion, R. Li, K.E. Waters, A review of reagents applied to rare-earth mineral flotation, Adv. Colloid Interface Sci. 279 (2020), 102142, https://doi.org/10.1016/j.cis.2020.102142.

[5] H.G. Dill, Pegmatites and aplites: their genetic and applied ore geology, Ore Geol. Rev. 69 (2015) 417–561, https://doi.org/10.1016/j.oregeorev.2015.02.022.

[6] S.M. Bulatovic, Beneficiation of zircon containing ores, in: Handbook of Flotation Reagents: Chemistry, Theory and Practice, Elsevier, Amsterdam, 2015, pp. 91–105.

[7] A. Jordens, Y.P. Cheng, K.E. Waters, A review of the beneficiation of rare earth element bearing minerals, Miner. Eng. 41 (2013) 97–114, https://doi.org/10.1016/j.mineng.2012.10.017.

[8] M.S. Celik, I. Can, R.H. Eren, Removal of titanium impurities from feldspar ores by new flotation collectors, Miner. Eng. 11 (1998) 1201–1208, https://doi.org/10.1016/S0892-6875(98)00106-X.

[9] G.B. Abaka-Wood, J. Addai-Mensah, W. Skinner, A study of selective flotation recovery of rare earth oxides from hematite and quartz using hydroxamic acid as a collector, Adv. Powder Technol. 29 (2018) 1886–1899, https://doi.org/10.1016/j.apt.2018.04.028.

[10] B.M. Antti, E. Forssberg, Pulp chemistry in industrial mineral flotation. Studies of surface complex on calcite and apatite surfaces using FTIR spectroscopy, Miner. Eng. 2 (1989) 217–227, https://doi.org/10.1016/0892-6875(89)90042-3.

[11] K.I. Marinakis, H.L. Shergold, The mechanism of fatty acid adsorption in the presence of fluorite, calcite and barite, Int. J. Miner. Process. 14 (1985) 161–176, https://doi.org/10.1016/0301-7516(85)90001-8.

[12] I.V. Filippova, L.O. Filippov, A. Duverger, V.V. Severov, Synergetic effect of a mixture of anionic and nonionic reagents: Ca mineral contrast separation by flotation at neutral pH, Miner. Eng. 66–68 (2014) 135–144, https://doi.org/10.1016/j.mineng.2014.05.009.

[13] B.M. Moudgil, R. Chanchani, Beneficiation of complex phosphate ores from South Florida by two stage conditioning process, XVth Int. Miner. Process. Congr. (1985) 357–366.

[14] J.V. Satur, B.P. Calabia, M. Hoshino, S. Morita, Y. Seo, Y. Kon, T. Takagi, Y. Watanabe, L. Mutele, S. Foya, Flotation of rare earth minerals from silicate–hematite ore using tall oil fatty acid collector, Miner. Eng. 89 (2016) 52–62, https://doi.org/10.1016/j.mineng.2016.01.004.

[15] J.L. Serra, A. Rodrigues, R.A. de Freitas, A.J.A. Meirelles, S.H. Darnet, L. Silva, Alternative sources of oils and fats from Amazonian plants: fatty acids, methyl tocols, total carotenoids and chemical composition, Food Res. Int. 116 (2019) 12–19. https://10.1016/j.foodres.2018.12.028.

[16] K.L.C. da Silva, M.M.C. da Silva, M.M. de Moraes, C.A.G. da Camara, M.L. dos Santos, C.W. Fagg, Chemical composition and acaricidal activity of essential oils from two species of the genus Bauhinia that occur in the Cerrado biome in Brazil, J. Essent. Oil Res. 32 (2020) 23–31. https://10.1080/10412905.2019.1662338.

[17] J.A. Flores, O. Konrad, C.R. Flores, N.T. Schroder, Inventory data on Brazilian Amazon′ s non-wood native biomass sources for bioenergy production, Data Brief 20 (2018) 1935–1941, https://doi.org/10.1016/j.dib.2018.09.050.

[18] J.A.E. de Carvalho, P.R.G. Brandão, A.B. Henriques, P.S. de Oliveira, R.Z.L. Cançado, G.R. da Silva, Selective flotation of apatite from micaceous minerals using patauá palm tree oil collector, Miner. Eng. 156 (2020), 106474, https://doi.org/10.1016/j.mineng.2020.106474.

[19] P. Oliveira, H. Mansur, A. Mansur, G.R. da Silva, A.E.C. Peres, Apatite flotation using pataua palm tree oil as collector, J. Mater. Res. Technol. 8 (2019) 4612–4619, https://doi.org/10.1016/j.jmrt.2019.08.005.

[20] P.R.M. Viana, A.C. Araujo, A.E.C. Peres, G.E.S. Valadão, Adsorção de misturas de coletores em silicatos, J. Rem. 59 (2006) 421–425, https://doi.org/10.1590/S0370-44672006000400012.

[21] Y. Xu, L. Xu, H. Wu, Z. Wang, K. Shu, S. Fang, Z. Zhang, Flotation and co–adsorption of mixed collectors octanohydroxamic acid/sodium oleate on bastnaesite, J. Alloys Compd. 819 (2020), 152948, https://doi.org/10.1016/j.jallcom.2019.152948.
[22] Pracaxi (Pentaclethra macroloba). https://www.amazonoil.com.br//(accessed May, 4, 2021).
[23] C.S. Chereh, M. Rudolph, T. Leistner, J. Gutzmer, U.A. Peuker, A review of rare earth minerals flotation: monazite and xenotime, Int. J. Min. Sci. Technol. 25 (2015) 877–883. https://10.1016/j.ijmst.2015.09.002.
[24] C.E. Stauffer, Funtional properties of fat ans oils, in: Fat and Oils, Eagan Press, Saint Paul, 1996, pp. 1–14.
[25] T.-W. Cheng, P.N. Holtham, T. Tran, Froth flotation of monazite and xenotime, Miner. Eng. 6 (1993) 341–351, https://doi.org/10.1016/0892-6875(93)90014-E.
[26] E.P. Heppard, A.J. Kinney, K.L. Stecca, G.H. Miao, Developmental and growth temperature regulation of two different microsomal [omega]-6 desaturase genes in soybeans, J. Plant Physiol. 110 (1996) 311–319. https://10.1104/pp.110.1.311.
[27] Y. Wang, Y. Feng, Q. Zhang, D. Lu, Y. Hu, Flotation separation of diaspore from aluminosilicates using commercial oleic acids of different iodine values, Int. J. Miner. Process. 168 (2017) 95–101, https://doi.org/10.1016/j.minpro.2017.09.013.
[28] P.G.S. Lédo, J.B.A. Paulo, R.F.S. Lima, P.R.G. Brandão, M. Vieira, Flotação de Calcita utilizando óleos vegetais regionais saponificados, XX Encontro Nacional de Tratamento de Minérios e Metalurgia Extrativa, 2004, pp. 61–68.
[29] L. Wang, W. Zhou, S. Song, H. Gao, F. Niu, J. Zhang, G. Ai, Selective separation of hematite from quartz with sodium oleate collector and calcium lignosulphonate depressant, J. Mol. Liq. 322 (2021). https://10.1016/j.molliq.2020.114502.
[30] Q. Cao, J. Cheng, S. Wen, C. Li, S. Bai, D. Liu, A mixed collector system for phosphate flotation, Miner. Eng. 78 (2015) 114–121, https://doi.org/10.1016/j.mineng.2015.04.020.
[31] Y. Zhang, Y. Hu, N. Sun, R. Liu, Z. Wang, L. Wang, W. Sun, Systematic review of feldspar beneficiation and its comprehensive application, Miner. Eng. 128 (2018) 141–152, https://doi.org/10.1016/j.mineng.2018.08.043.
[32] A. Pattanaik, R. Venugopal, Investigation of adsorption mechanism of reagents (surfactants) system and its applicability in iron ore flotation – an overview, Colloid Interface Sci. Commun. 25 (2018) 41–65. https://10.1016/j.colcom.2018.06.003.
[33] G.B. Abaka-Wood, J. Addai-Mensah, W. Skinner, Selective flotation of rare earth oxides from hematite and quartz mixtures using oleic acid as a collector, Int. J. Miner. Process. 169 (2017) 60–69. https://10.1016/j.minpro.2017.10.002.
[34] C.D. Anderson, P.R. Taylor, C.G. Anderson, Rare earth flotation fundamentals: a review, Am. J. Eng. Res. 6 (2017) 155–166.
[35] A.R.S. de Medeiros, C.A.M. Baltar, Importance of collector chain length in flotation of fine particles, Miner. Eng. 122 (2018) 179–184. https://10.1016/j.mineng.2018.03.008.
[36] T.-W. Cheng, A.C. Partridge, T. Tran, P.L.M. Wong, The surface properties and flotation behaviour of xenotime, Miner. Eng. 7 (1994) 1085–1098, https://doi.org/10.1016/0892-6875(94)90001-9.
[37] K.H. Rao, K.S.E. Forssberg, Interactions of anionic collectors in flotation of semi-soluble salt minerals, in: Innovations in Flotation Technology, Springer, 1992, pp. 331–356.
[38] B.M. Antti, E. Forssberg, Pulp chemistry in calcite flotation. Modelling of oleate adsorption using theoretical equilibrium calculations, Miner. Eng. 2 (1989) 93–109, https://doi.org/10.1016/0892-6875(89)90068-X.
[39] B.M. Moudgil, H. Soto, P. Somasundaran, Adsorption of surfactants on minerals, in: Reagents in Mineral Technology, Routledge, 2018, pp. 79–104.
[40] B. McFadzean, T. Marozva, J. Wiese, Flotation frother mixtures: decoupling the sub-processes of froth stability, froth recovery and entrainment, Miner. Eng. 85 (2016) 72–79, https://doi.org/10.1016/j.mineng.2015.10.014.
[41] D.J. Bradshaw, P.J. Harris, C.T. O'Connor, Synergistic interactions between reagents in sulphide flotation, J. South. Afr. Inst. 98 (1998) 189–193. https://hdl.handle.net/10520/AJA0038223X_2481.
[42] H. Jiang, W. Ji, Q. Yang, L. Xu, C. Zhao, Y. Hu, Synergistic adsorption and flotation of new mixed cationic/nonionic collectors on muscovite, Miner. Eng. 7 (2017) 74, https://doi.org/10.3390/min7050074.
[43] K.H. Rao, R.K. Dwari, S. Lu, A. Vilinska, P. Somasundaran, Mixed anionic/non-ionic collectors in phosphate gangue flotation from magnetite fines, J. Open Min. Process 4 (2011). https://10.2174/1874841401104010014.
[44] G.B. Abaka-Wood, J. Addai-Mensah, W. Skinner, A study of flotation characteristics of monazite, hematite, and quartz using anionic collectors, Int. J. Miner. Process. 158 (2017) 55–62, https://doi.org/10.1016/j.minpro.2016.11.012.
[45] J.T. Kloprogge, B.J. Wood, Chemical bonding and electronic structures of microcline, orthoclase and the plagioclase series by X-ray photoelectron spectroscopy, Spectrochim. Acta Mol. Biomol. Spectrosc. 137 (2015) 711–716, https://doi.org/10.1016/j.saa.2014.08.120.
[46] B. Gong, P. Wu, B. Ruan, Y. Zhang, X. Lai, L. Yu, Y. Li, Z. Dang, Differential regulation of phenanthrene biodegradation process by kaolinite and quartz and the underlying mechanism, J. Hazard Mater. 349 (2018) 51–59, https://doi.org/10.1016/j.jhazmat.2018.01.046.
[47] J. Wang, Z. Wang, L. Yang, G. Yang, C. Miao, P. Lv, Natural albite as a novel solid basic catalyst for the effective synthesis of biodiesel: characteristics and performance, Energy J. 141 (2017) 1650–1660, https://doi.org/10.1016/j.energy.2017.11.086.
[48] H. Sahoo, S.S. Rath, B. Das, B.K. Mishra, Flotation of quartz using ionic liquid collectors with different functional groups and varying chain lengths, Miner. Eng. 95 (2016) 107–112, https://doi.org/10.1016/j.mineng.2016.06.024.
[49] L.O. Filippov, V.V. Severov, I.V. Filippova, Mechanism of starch adsorption on Fe–Mg–Al-bearing amphiboles, Int. J. Miner. Process. 123 (2013) 120–128, https://doi.org/10.1016/j.minpro.2013.05.010.
[50] M.R. Rafiuddin, E. Mueller, A.P. Grosvenor, X-ray Spectroscopic Study of the electronic structure of monazite-and xenotime-type rare-earth phosphates, J. Phys. Chem. C 118 (2014) 18000–18009, https://doi.org/10.1021/jp5051996.
[51] N. Gunasekaran, N. Bakshi, C.B. Alcock, J.J. Carberry, Surface characterization and catalytic properties of perovskite type solid oxide solutions, La0. 8Sr0. 2BO3 (B= Cr, Mn, Fe, Co or Y), Solid State Ionics 83 (1996) 145–150, https://doi.org/10.1016/0167-2738(95)00232-4.
[52] H. Wu, J. Wang, Z. Wang, D.R. Fisher, Y. Lin, Apoferritin-templated yttrium phosphate nanoparticle conjugates for radioimmunotherapy of cancers, J. Nanosci. Nanotechnol. 8 (2008) 2316–2322. https://10.1166/jnn.2008.177.
[53] P.S. Oliveira, Caracterização do óleo de patauá e utilização para obtenção de um reagente coletor para a flotação de minério fosfático, Doctoral thesis, Universidade Federal de Minas Gerais, 2017.
[54] J. Luo, X.J. Chen, Research into the recovery of high-grade rare-earth concentrate from Baotou Complex iron ores, China, Miner. Process. Extr. Metall. (IMM Trans. Sect. C) (1984) 663–675.
[55] D.W. Fuerstenau, C. Pradip, Mineral flotation with hydroxamate collectors, in: Reagents in the Minerals Industry, IMM London, 1984, pp. 161–168.